A 121.8dB Dynamic Range CMOS Image Sensor using Pixel-Variation-Free Midpoint Potential Drive and Overlapping Multiple Exposures

Yusuke Oike, Atsushi Toda, Tadayuki Taura, Akihiko Kato,
Hiroki Sato, Masanori Kasai and Tadakuni Narabu

Sony Corporation
4–14–1 Asahi-cho, Atsugi, Kanagawa, 243-0014 Japan
Phone: +81–46–202–7953, Fax: +81–46–230–6170
E-mail: Yusuke.Oike@jp.sony.com

Abstract

This paper presents a wide dynamic range CMOS image sensor using a pixel-variation-free midpoint potential drive with a double midpoint shutter. No degradation of the sensitivity is seen due to continuing charge integration. The double midpoint shutter suppresses the fixed pattern noise of short-exposure images and realizes high linearity throughout the full scale. We have developed a 2M pixel prototype using a 0.18 μm CMOS process with three 90 nm Cu layers. Wide dynamic range operation up to 121.8 dB has been successfully demonstrated.

Introduction

Dynamic range is a key performance specification of an image sensor and there have been various approaches to extending it [1]–[8]. However, these are not preferable for color images due to nonlinearity [1]–[3] or not applicable for small pixel structures because of their complex pixel circuits [3]–[5]. Multi-sampling is a well-known approach to linear dynamic range extension. In recent years, high-speed CMOS image sensors have been developed [6, 9] which can realize a multi-sampling wide dynamic range with high pixel resolutions. On the other hand, the conventional technique of multiple exposures decreases the sensitivity because of the split and divided exposure terms. That is, the minimum required illumination increases in exchange for dynamic range.

This paper presents a wide dynamic range CMOS image sensor using a pixel-variation-free midpoint potential drive with a double midpoint shutter. It provides multiple images of several short exposures in addition to an image at full exposure by continuing charge integration. There is no degradation of the sensitivity in the wide dynamic range operation unlike the well-known multiple-exposure technique such as [6]. This technique concurrently suppresses the fixed pattern noise in short-exposure images resulting from inter-pixel variations of device characteristics. Furthermore the double midpoint shutter achieves high linearity throughout the full range, which is its major advantage over the conventional techniques using midpoint drives [7, 8].

Wide Dynamic Range Operation

Figure 1 shows a block diagram and simplified schematics illustrating our wide dynamic range CMOS image sensor using a pixel-variation-free midpoint potential drive. It consists of a pixel array, row decoders and drivers with a midpoint potential driver, column CDS circuits with a sample and hold (S&H) function, and horizontal scanners. As peripherals, the sensor has a controller, a regulator to generate the midpoint voltage, and analog front ends (AFE). The pixel circuit has three transistors as described in [10]. The cost of the additional circuit, for the wide dynamic range operation, is only that of a row driver extension and a regulator for the midpoint voltage supply. Note that the present technique is also applicable to a small pixel structure such as [11].

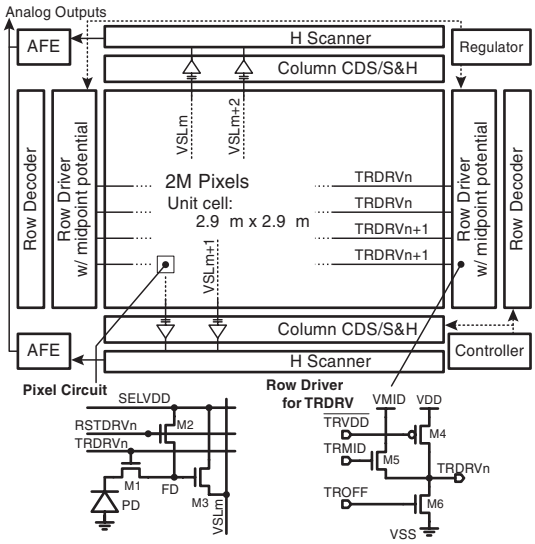

Fig. 1 Block diagram and simplified schematics.

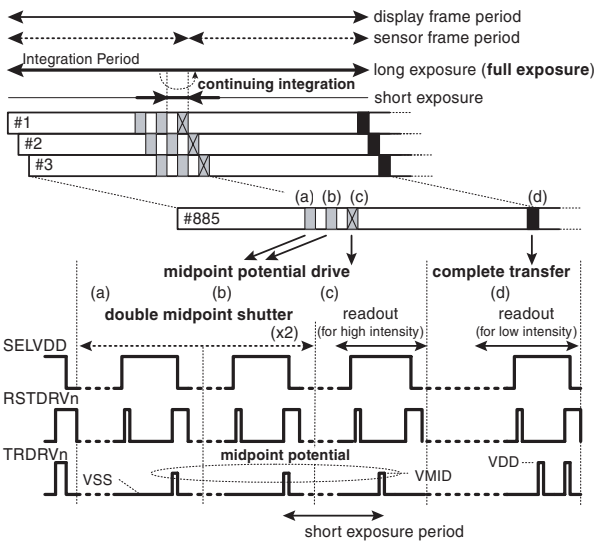

Fig. 2 Timing diagram.

Figure 2 illustrates the timing diagram of the overlapping multiple exposures using the midpoint potential drive. Multiple sensor frames are assigned to a display frame period, then the midpoint voltage of $VMID$ is repeatedly supplied to the charge transfer gate of $TRDRV_n$ during the full charge integration of the display frame period. The first two midpoint drives are used

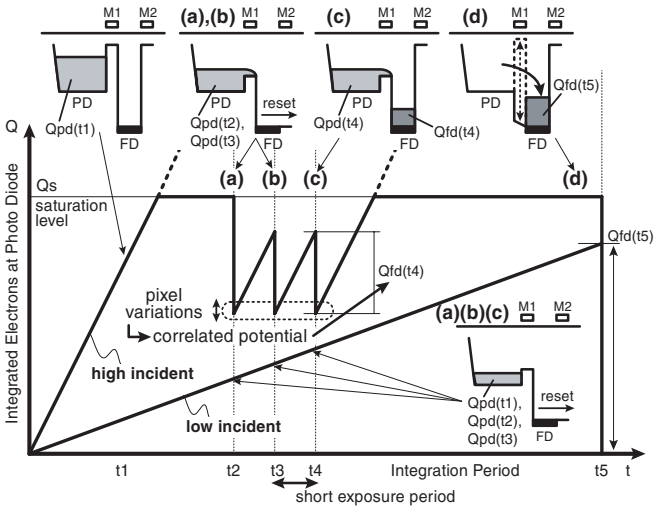

Fig. 3 Potential diagram of overlapping multiple exposures.

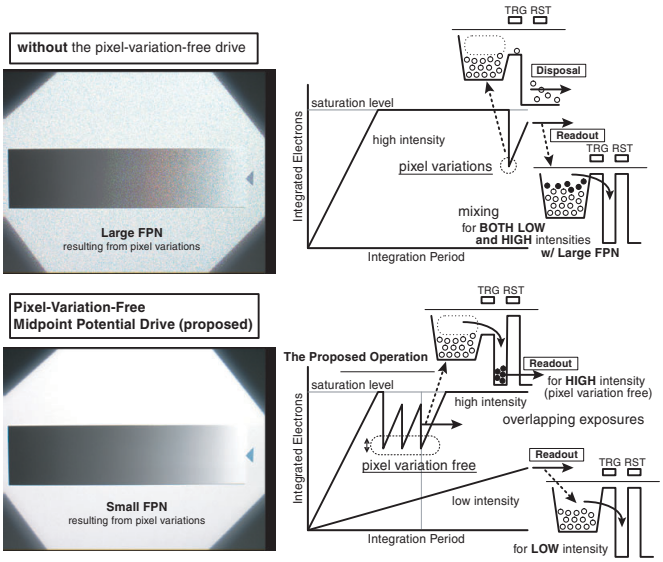

Fig. 4 Impact of pixel variations.

to make a double midpoint shutter, which sets the short exposure time and suppresses the FPN resulting from variations in device characteristics and supply voltages. The double midpoint shutter is provided from the relative timings (a) and (b) in Fig. 2. The last midpoint drive provides the image from the short exposure at the timing of (c). Finally, the complete charge transfer provides the image from the full exposure at the timing of (d) since the midpoint potential drives then allow continuation with charge integration for the low-intensity incident light.

Figure 3 is the potential diagram of overlapping multiple exposures. At a pixel with low-intensity incident light, the charge integration continues without a charge transfer by the midpoint potential drives. On the other hand, a partial charge transfer comes via the midpoint potential drives when the pixel receives high-intensity incident light which finally saturates it within the full integration time. The double midpoint shutter guarantees correlation in the potential between $Q_{pd}(t3)$ and $Q_{pd}(t4)$. Therefore the transferred charge of $Q_{fd}(t4)$ is free from pixel variations such as those caused by the threshold voltage of the transfer gates, the uneven distribution of impurities, the supplied midpoint voltage level, and the pulse settling time of $TRDRV_n$ as shown in Fig. 4.

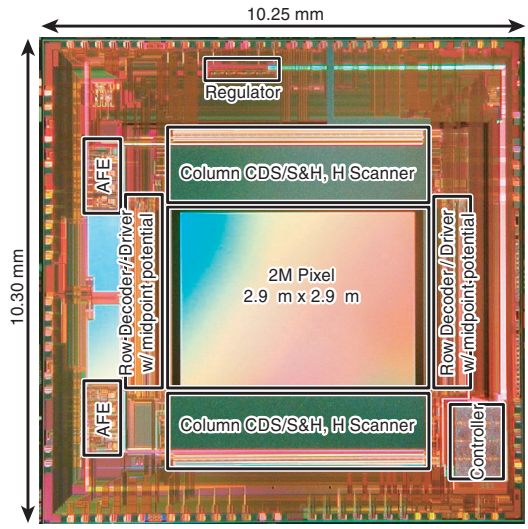

Fig. 5 Chip microphotograph.

Table 1 Chip Characteristics.

Process	0.18 μm CMOS + 90 nm 3 Cu layers
Die size	10,250 μm (H) $\times$ 10,300 μm (V)
Supply voltage	3.3 V / 1.5 V
Num. effective pixels	2 M pixels
Pixel size	2.9 μm $\times$ 2.9 μm
Max. frame rate	60 frames/s
RMS random noise	6.5 e-$_{rms}$ at 60 frames/s at dark level
RMS fixed pattern noise	2.0 e-$_{rms}$ at 60 frames/s at dark level
Conversion gain	88 μV/e-
Dynamic range	62.8 dB (normal operation)
Max. dynamic range	121.8 dB at 15 fps display rate

At the timing of (a) and (b) in Fig. 3, the transferred charges are reset without a readout operation. Then, the transferred charge of $Q_{fd}(t4)$ is read out as an image of the short exposure at the timing of (c). The integration period between (b) and (c) defines the short exposure time. The initial potential at (b), which is a condition just before the partial charge transfer at the starting point of the short exposure, needs to be correlated with the initial potential at (c) in order to get the exact charge integrated during the short exposure time. Therefore the first shutter is provided at the timing of (a) which is previous to the starting point of short exposure, and the time interval between (a) and (b) is the same period of the short exposure time. The double midpoint shutter makes the initial potential at (b) correlated to the initial potential at (c) as shown in Fig. 3. It achieves two advantages over conventional techniques using a midpoint drive [7, 8]. One is higher linearity throughout the full range. The linearity is not affected by variations of the midpoint voltage, since the offset is canceled due to the potential correlation. The other is a wider dynamic range because our technique is capable of cascading dynamic range extensions owing to the higher linearity and the offset canceling. Finally, the transferred charge of $Q_{fd}(t5)$ is read out as an image of the full exposure at the timing of (d).

Multiple sequences of the midpoint drives are iteratively applicable with arbitrary exposure times during the full exposure period. The overlapping multiple exposures can provide several images with different sensitivities in addition to that of the maximum sensitivity.

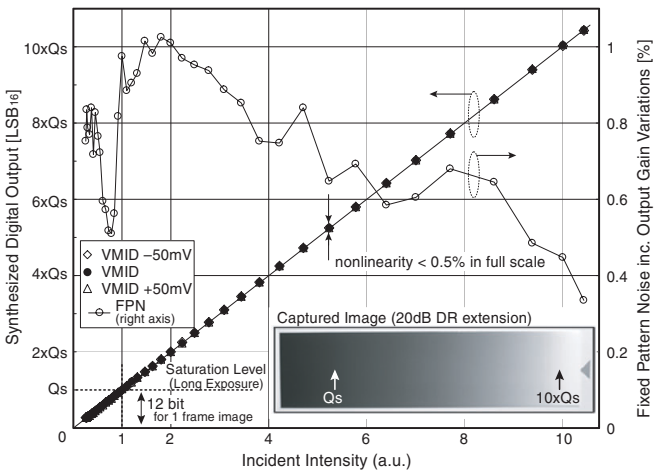

Fig. 6 Linearity and fixed pattern noise.

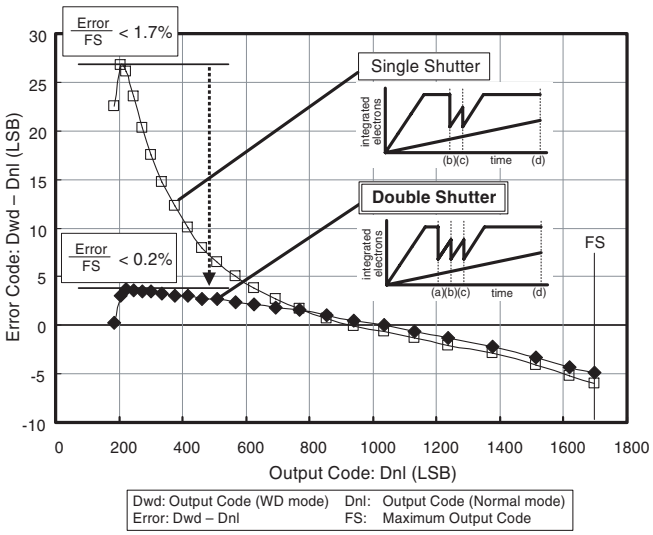

Fig. 7 Error suppression by the double midpoint shutter.

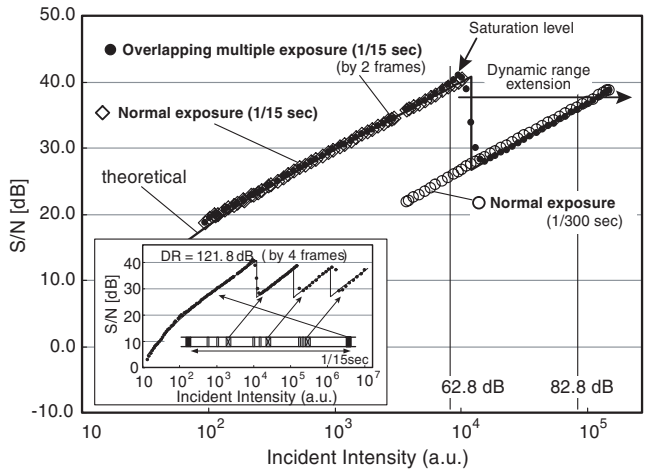

Fig. 8 Signal-to-noise ratio.

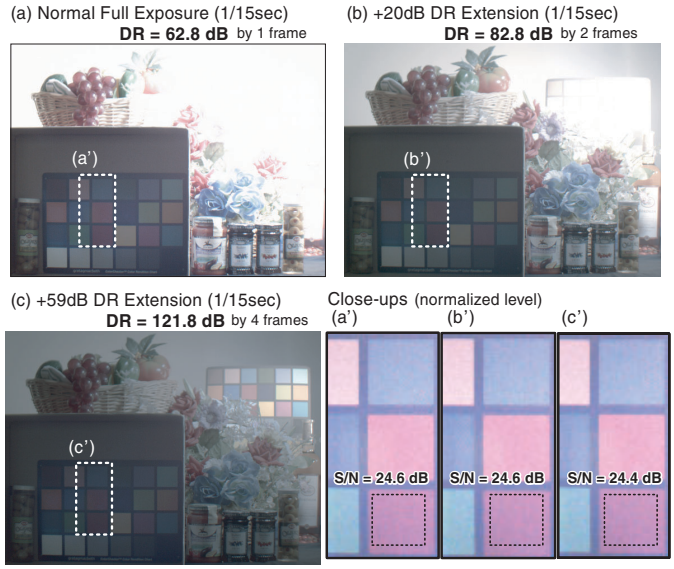

Fig. 9 Reproduced images.

Chip Implementation

We designed and fabricated a 2M pixel CMOS image sensor, shown in Fig. 5, using a 0.18 μm CMOS process with three 90 nm Cu layers. The die size was $10{,}250 \times 10{,}300\ \mu\text{m}^2$. The supply voltages were 3.3 V for analog parts and 1.5 V for digital parts. The pixel size was 2.9 μm × 2.9 μm. The random noise (RN) was 6.5 e-$_{rms}$ and the FPN was 2.0 e-$_{rms}$ at the dark level. The innate dynamic range was 62.8 dB. The chip characteristics are summarized in Table 1.

Measurement Results

Figure 6 shows the measured results for the linearity and the fixed pattern noise in a 20 dB dynamic range extension by 2 frames. The midpoint voltages were set to $VIMD$, $VMID - 50$ mV, and $VMID + 50$ mV, respectively, to verify the robustness of device with the pixel-variation-free midpoint potential drive. Here, the error is defined as $|D_{wd} - D_{nl}|/FS$, where D_{wd} is the output data of the wide dynamic range operation, D_{nl} is that of a normal short-exposure operation, and FS is the full code. An error of less than 0.5 % of the full scale was found and this value was not affected by the variations of the midpoint voltage; as expected as the connecting point is provided by the sum of the long- and short-exposure output codes and any offset in the short-exposure output will be reduced due to the potential correlation.

The FPN at the dark level was 2.0 e-$_{rms}$, just as it was in the innate specification. The FPN including output gain variations was less than 1.1 % due to the double midpoint shutter. The random noise at the dark level was 6.5 e-$_{rms}$ as the same as the innate device. A captured image with 20 dB extension is inserted into Fig. 6. There is no obvious solarization or posterization.

The double midpoint shutter effectively suppresses the offset error as shown in Fig. 7. Here the error code of $|D_{wd} - D_{nl}|$ is plotted for the case of 18 dB dynamic range extension. In a single midpoint shutter operation, where the first midpoint shutter is excluded, the offset error was found to be 1.7 % at the boundary of dynamic range extension. This offset error at the boundary leads to a color shift after the white balance processing. The double midpoint shutter reduces this offset error to 0.2 %. The high linearity provides a good gradation sequence without any color shift.

The measured signal-to-noise ratio is plotted in Fig. 8. The S/N of overlapping multiple exposures is in excellent agreement with a normal exposure using the full integration time in the innate dynamic range of 62.8 dB. The S/N follows that of a normal short exposure in the extended dynamic range. In this case, the interval of midpoint potential drives was 1/300 sec, and the S/N was at the level of a 1/300-sec normal short expo-

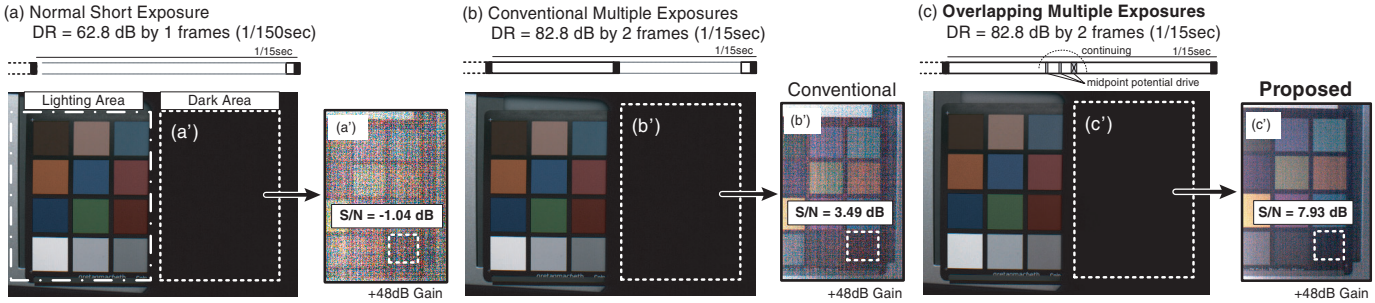

Fig. 10 Comparison with the conventional multiple exposures.

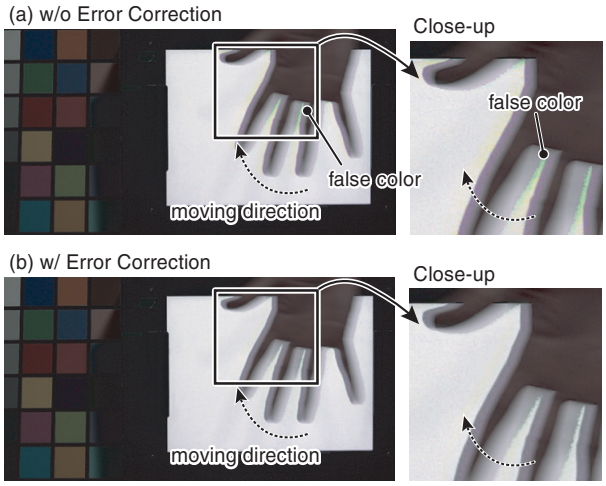

Fig. 11 A sample image of a moving target object.

sure. The present technique is capable of cascading dynamic range extensions according to the ratio of the sensor frame rate to the display frame rate. The prototype image sensor achieved a 121.8 dB dynamic range by 4 frames at a 15 fps display rate as shown by the inserted plot in Fig. 8.

Figure 9 shows reproduced color images. A normal exposure of 1/15 sec provided the maximum sensitivity at a display rate of 15 fps. Figure 9 (a) is, however, saturated because the dynamic range of 62.8 dB was not enough for the high contrast scene. Figure 9 (a') is a close-up. Figure 9 (b) and (c) are reproduced images of 82.8 dB by 2 frames and 121.8 dB by 4 frames, respectively, using overlapping multiple exposures. The S/N in the dark region agrees with (a') as presented in the close-ups of (b') and (c'). Figure 10 shows a comparison with the conventional multiple exposure technique. The present technique achieved a 121.8 dB linear dynamic range without either sensitivity loss in a dark region or visible FPN in a bright region. Thus, we can say that this highly linear and wide dynamic range operation is more suitable for color and high-pixel-resolution image sensing than conventional techniques.

We have also developed a signal processing algorithm to reduce false color for a moving target object. In the wide dynamic range technique, a reproduced image is a composite image using several integration periods. Therefore, several moving target objects against a static background would be captured over different integration periods for a high contrast scene. Figure 11 is a sample image of such a moving target object. Some false colors were seen to at the boundaries of the moving object. Our false color reduction algorithm successfully detects the error region and effectively suppresses the false color as shown in Fig. 11.

Conclusions

We have presented a 121.8 dB dynamic range CMOS image sensor using pixel-variation-free midpoint potential drives and overlapping multiple exposures. The pixel-variation-free midpoint potential drive provides multiple images of several short exposures, in addition to an image of the full exposure by continuing charge integration. There is no sensitivity loss, even in wide dynamic range operation, since this technique makes efficient use of the full exposure time. Furthermore, the double midpoint shutter concurrently suppresses the fixed pattern noise, resulting from inter-pixel variations of device characteristics, of short-exposure images. Small pixel configurations are no barrier for the wide dynamic range operation and we believe that the present technique is applicable to various fields of image sensing.

References

[1] G. G. Storm *et al.*, "Combined Liner-Logarithmic CMOS Image Sensor," *IEEE ISSCC Dig. Tech. Papers*, pp.112–113, Feb. 2004.

[2] K. Hara *et al.*, "A Linear-Logarithmic CMOS Sensor with Offset Calibration Using an Injected Charge Signal," *IEEE ISSCC Dig. Tech. Papers*, pp.354–355, Feb. 2005.

[3] N. Akahane *et al.*, "A 200dB Dynamic Range Iris-less CMOS Image Sensor with Lateral Overflow Integration Capacitor using Hybrid Voltage and Current Readout Operation," *IEEE ISSCC Dig. Tech. Papers*, pp.300–301, Feb. 2006.

[4] D. Yang *et al.*, "A 640 × 512 CMOS Image Sensor with Ultra Wide Dynamic Range Floating-Point Pixel-Level ADC," *IEEE ISSCC Dig. Tech. Papers*, pp.308–309, Feb. 1999.

[5] S. Sugawa *et al.*, "A 100dB Dynamic Range CMOS Image Sensor Using a Lateral Overflow Integration Capacitor," *IEEE ISSCC Dig. Tech. Papers*, pp.352–352, Feb. 2005.

[6] M. Mase *et al.*, "A 19.5b Dynamic Range CMOS Image Sensor with 12b Column-Parallel Cyclic A/D Converters," *IEEE ISSCC Dig. Tech. Papers*, pp.352–352, Feb. 2005.

[7] S. Decker *et al.*, "A 256×256 CMOS Imaging Array with Wide Dynamic Range Pixels and Column-Parallel Digital Output," *IEEE J. Solid-State Circuits*, vol.33, no.12, pp.2081–2091, Dec. 1998.

[8] Y. Egawa *et al.*, "A 1/2.5 inch 5.2Mpixel, 96dB Dynamic Range CMOS Image Sensor with Fixed Pattern Noise Free, Double Exposure Time Read-Out Operation," *in Proc. IEEE Asian Solid-State Circuits Conf.*, pp.135–138, Nov. 2006.

[9] Y. Nitta *et al.*, "High-Speed Digital Double Sampling with Analog CDS on Column Parallel ADC Architecture for Low-Noise Active Pixel Sensor," *IEEE ISSCC Dig. Tech. Papers*, pp.500–501, Feb. 2006.

[10] K. Mabuchi *et al.*, "CMOS Image Sensor Using a Floating Diffusion Driving Buried Photodiode," *IEEE ISSCC Dig. Tech. Papers*, pp.112–113, Feb. 2004.

[11] M. Mori *et al.*, "A 1/4in 2M Pixel CMOS Image Sensor with 1.75 Transistor/Pixel," *IEEE ISSCC Dig. Tech. Papers*, pp.110–111, Feb. 2004.